2624 *Inorg. Chem.* **2010**, *49*, 2624–2629
DOI: 10.1021/ic901551t

Inorganic Chemistry
Article

Functionalized O-Alkyldithiocarbonates: A New Class of Ligands Designed for Luminescent Heterometallic Materials

Radu F. Semeniuc,*,† Thomas J. Reamer,† Jonathan P. Blitz,† Kraig A. Wheeler,† and Mark D. Smith‡

†*Department of Chemistry, Eastern Illinois University, Charleston, Illinois 61920, and*
‡*Department of Chemistry and Biochemistry, University of South Carolina, Columbia, South Carolina 29208*

Received August 4, 2009

The new ligand 4-PyCH$_2$OCS$_2$Na, that combines two different donor groups in one molecule (a soft $-CS_2^-$ group and a hard pyridine moiety), has been synthesized. The ligand coordinates to a $[(bipy)Re(CO)_3]^+$ center in a monodentate fashion through one of its soft sulfur atoms, leaving the hard pyridine terminus free for further coordination chemistry. Using a Ni(II) dithiophosphonate linker, the heterometallic $\{[CH_3OCH_2CH_2OP(An)S_2]_2Ni\}[4\text{-}PyCH_2OCS_2Re(bipy)(CO)_3]_2$ complex is obtained, through the coordination of two pyridine groups to the Ni(II) center. This simple, high-yield stepwise strategy toward heterometallic complexes could be easily transferable to other 1,1-dithiolate ligands and used in combination with a large variety of luminescent metallic systems.

Introduction

O-Alkyldithiocarbonates ($RO-CS_2^-$) represent an important class of 1,1-dithiolate ligands, along with dithiocarbamates ($R_2N-CS_2^-$), dithiocarboxylates ($R-CS_2^-$), dithiophosphonates ($R'(RO)-PS_2^-$), and other related phosphor-1,1-dithiolate ligands. Metallic derivatives of $RO-CS_2^-$ ligands have been known since 1815, when they were first prepared by Zeise, who also termed them xanthates, a name derived from the Greek *xanthos* (yellow), owing to the yellow color of lead xanthates.[1] For about 100 years, their applications were limited to the vulcanization of rubber and as fungicides, and only in the early 1900s did these compounds start to be used on a large scale as flotation agents in metallurgy.[2] Recently, applications to carbon−carbon bond formation through a degenerative radical mechanism were associated with the xanthate compounds.[3]

Their synthetic and structural chemistry witnessed increased attention through the pioneering work of Hoskins and Winter and others,[4] and lately, extensive structural analyses performed by Haiduc and Tiekink, showed that they can coordinate to metal atoms (Chart 1) in a monodentate (a), isobidentate (b), or anisobidentate (c) fashion. Bimetallic bridging also occurs through sulfur atoms (d, e), but occasionally the oxygen atom may become involved (f).[5] Further, the presence of soft Lewis acidic centers on these ligands, i.e., sulfur, gives rise to the possibility of supramolecular association in the crystalline phase. Thus, hypervalent interactions or secondary bonds are often observed, leading to interesting self-assembled supramolecular architectures.[5−7]

Surprisingly, in spite of years of chemistry, there are no significant reports of xanthate ligands functionalized with additional donor groups,[8a] that would expand their coordination capabilities. By modifying the backbone of these soft ligands with a second donor set (for instance with hard donors such as pyridine-based groups), it should be possible to take advantage of their rich coordination patterns and differences between the coordination preferences of sulfur atoms for "soft metals" and of pyridine-based groups for "hard metals" to design and prepare new heterometallic species. An added benefit of this approach arises from the negatively charged $-CS_2$ group: in a first step, a suitable metal system would be inserted at the "soft end" of the ligand, since it will also be a charge driven process, while keeping the "hard end" free for further

*To whom correspondence should be addressed. E-mail: rsemeniuc@eiu.edu.

(1) Zeise, W. C. *Rec. Mem. Acad. R. Sci. Copenhagen* **1815**, *1*, 1.
(2) Abramov, A. A.; Forssberg, K. S. E. *Miner. Process. Extr. Metall. Rev*. **2005**, *26*, 77.
(3) Quiclet-Sire, B.; Zard, S. Z. *Top. Curr. Chem*. **2006**, *264*, 201.
(4) (a) Winter, G. *Rev. Inorg. Chem*. **1980**, *2*, 253. (b) Tiekink, E. R. T.; Winter, G. *Rev. Inorg. Chem*. **1992**, *12*, 183. (c) Hoskins, B. F.; Pannan, C. D. *Chem. Commun*. **1975**, 408. (d) Dakternieks, D.; Di Giacomo, R.; Gable, R. W.; Hoskins, B. F. *J. Am. Chem. Soc*. **1988**, *110*, 6753.
(5) Tiekink, E. R. T.; Haiduc, I. *Prog. Inorg. Chem*. **2005**, *54*, 127.
(6) Garje, S. S.; Jain, V. K. *Coord. Chem. Rev*. **2003**, *236*, 35.
(7) (a) Casas, J. S.; Castineiras, A.; Haiduc, I.; Sanchez, A.; Semeniuc, R. F.; Sordo, J. *J. Mol. Struct*. **2003**, *656*, 225. (b) Casas, J. S.; Castellano, E. E.; Ellena, J.; Haiduc, I.; Sanchez, A.; Semeniuc, R. F.; Sordo, J. *Inorg. Chim. Acta* **2002**, *329*, 71.
(8) (a) Krebs, H; Weber, E. F.; Fassbender, H. *Z. Anorg. Allg. Chem*. **1954**, *276*, 128. (b) Watkins, S. E.; Craig, D. C.; Colbran, S. B. *J. Chem. Soc., Dalton Trans*. **2002**, 2423. (c) Graf, E.; Hosseini, M. W.; Ruppert, R. *Tetrahedron Lett*. **1994**, *35*, 7779. (d) Sun, X.; Johnson, D. W.; Caulder, D. L.; Raymond, K. N.; Wong, E. H. *J. Am. Chem. Soc*. **2001**, *123*, 2752. (e) Silva, R. M.; Gwengo, C.; Lindeman, S. V.; Smith, M. D.; Gardinier, J. R. *Inorg. Chem*. **2006**, *45*, 10998. (f) Wilton-Ely, J. D. E. T.; Solanki, D.; Knight, E. R.; Holt, K. B.; Thompson, A. L.; Hogarth, G. *Inorg. Chem*. **2008**, *47*, 9642.

Published on Web 02/17/2010

Chart 1. Coordination Modes of the Xanthate Ligands

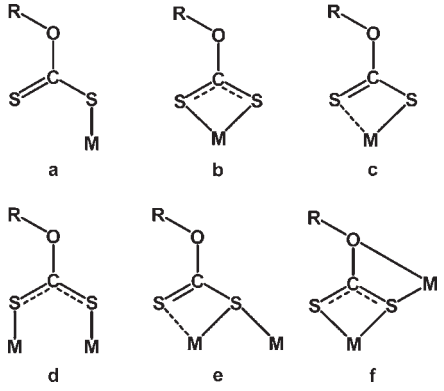

coordination chemistry. A second step would involve the insertion of a second metallic species, at the "hard end" of the ligand. While variations of multitopic ligands incorporating hard and/or soft binding sites have been widely used to create luminescent polymetallic arrays,[8b−f,9] this approach has only been recently applied to the 1,1-dithiolate class of ligands by preparing symmetrical ditopic dithiocarbamate ligands.[10] Examples of dissymmetric ditopic ligands incorporating 1,1-dithiolates as one of the donor sets and functionalized with a different secondary donor group are still rare.[8a] Therefore, we started a project to synthesize heterometallic architectures by applying the hard−soft acid base (HSAB) principles to the xanthate class of ligands, according to the synthetic strategy pictured in Scheme 1. Reported here are the synthesis and characterization of a backbone functionalized xanthate ligand, its monometallic derivative, and their use in the preparation of a luminescent heterometallic compound consisting of a heteroleptic xanthate−dithiophosphonate ligand system.

Results and Discussion

Starting from 4-pyridinemethanol, the 4-$PyCH_2OCS_2Na$ ligand (**L1**) was prepared in 93% yield as a pale yellow powder, by deprotonating the pyridine alcohol with NaH, followed by the CS_2 insertion reaction.[4,7] The ligand is air and moisture stable, and soluble in water, alcohols, and acetone and insoluble in halogenated solvents and ethers.

To test the selective coordination behavior of **L1** toward different metallic centers, we chose the $[(bipy)Re(CO)_3]^+$ fragment to be the [M1] metallic system for two important reasons.

Scheme 1. Synthetic Strategy toward Heterometallic Architectures Based on Pyridine Functionalized O-Alkyldithiocarbonates[a]

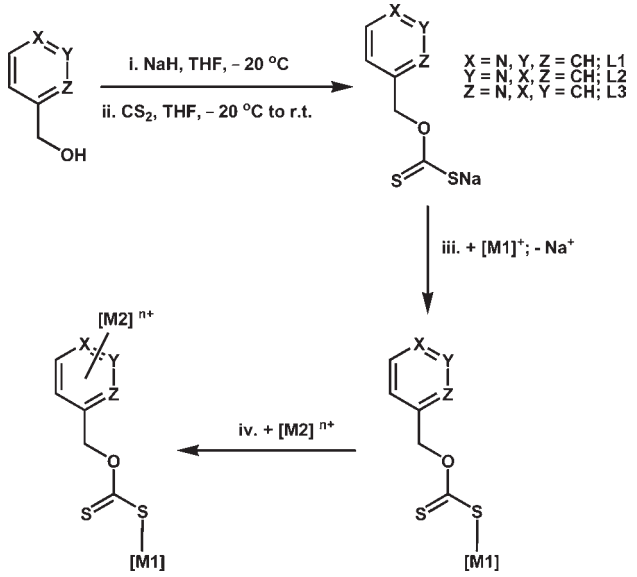

[a] [M1] and [M2] represent two different metallic systems.

First, this system consists of nonlabile ligands bonded to a metallic(I) center with only one open coordination site, a characteristic that would "force" **L1** to bond to it only through the negatively charged $-CS_2$ set, and leaving the pyridine end free for further coordination chemistry. Second, the incorporation of luminescent groups such as $[Re(bipy)(CO)_3]$ fragments into metal-based architectures,[9] especially into heteronuclear transition metal complexes,[9b,e,g,h] is of particular interest because of the rich spectroscopic and photophysical behavior associated with these complexes, with potential applications as devices at the molecular level.[9d−f,11] These heterometallic species are frequently isolated in low yields, and sometimes after challenging synthetic steps.[9g−j] Most of the organic ligands used in the preparation of such heterometallic luminescent species consist either of pyridine-based moieties or of alkynyl groups, since these donor sets allow to some extent a stepwise approach to the desired goal, which is linking two different metals within one molecule.

The metathesis reaction of **L1** and $[Re(bipy)(CO)_3(NCCH_3)](O_3SCF_3)$ ([**Re**]) in acetone in a 1:1 ratio yields, after removal of NaO_3SCF_3 and volatiles, an orange solid in 82% yield, identified as 4-$PyCH_2OCS_2Re(bipy)(CO)_3$ (**1**). Crystallization of **1** from CH_2Cl_2/hexanes afforded crystals suitable for X-ray diffraction studies. The compound crystallizes in the space group $P\bar{1}$, and the asymmetric unit consists of one 4-$PyCH_2OCS_2Re(bipy)(CO)_3$ complex (**1**) and half of a CH_2Cl_2 molecule. The molecular structure of **1** is presented in Figure 1a and consists of a $Re(bipy)(CO)_3$ core, with **L1** coordinated to the Re(I) in a monodentate fashion through one sulfur atom, with the second sulfur atom oriented away from the Re(I) center. The carbonyl groups are in a *fac* arrangement, and the geometry about the Re(I) atom is distorted octahedral (see Figure 1 for selected bond distances and angles), with distortions arising from the restraints imposed by the "bite" angle of the chelate bipyridine ring.

(9) (a) Yam, V. W.-W.; Lau, V. C.-Y.; Cheung, K.-K. *J. Chem. Soc., Chem. Commun.* **1995**, 259. (b) Yam, V. W.-W.; Pui, Y.-L.; Wong, K. M.-C.; Cheung, K.-K. *Chem. Commun.* **2000**, 1751. (c) Yam, V. W.-W.; Wong, K. M.-C.; Cheung, K.-K. *Organometallics* **1997**, *16*, 1729. (d) Chong, S. H.-F.; Lam, S. C.-F.; Yam, V. W.-W.; Zhu, N.; Cheung, K.-K.; Fathallah, S.; Costuas, K.; Halet, J.-F. *Organometallics* **2004**, *23*, 4924. (e) Kumar, A.; Sun, S.-S.; Lees, A. J. *Coord. Chem. Rev.* **2008**, *252*, 922. (f) Sun, S.-S.; Lees, A. J. *J. Am. Chem. Soc.* **2000**, *122*, 8956. (g) Packheiser, R.; Ecorchard, P.; Rüffer, T.; Lang, H. *Chem.—Eur. J.* **2008**, *14*, 4948. (h) Packheiser, R.; Ecorchard, P.; Rüffer, T.; Lang, H. *Organometallics* **2008**, *27*, 3534. (i) Coe, B. J.; Fitzgerald, E. C.; Helliwell, M.; Brunschwig, B. S.; Fitch, A. G.; Harris, J. A.; Coles, S. J.; Horton, P. N.; Hursthouse, M. B. *Organometallics* **2008**, *27*, 2730. (j) Packheiser, R.; Ecorchard, P.; Rüffer, T.; Lohan; Braüer, B. M.; Justaud, F.; Lapinte, C.; Lang, H. *Organometallics* **2008**, *27*, 3444.

(10) (a) Macgregor, M. J.; Hogarth, G.; Thompson, A. L.; Wilton-Ely, J. D. E. T. *Organometallics* **2009**, *28*, 197. (b) Cookson, J.; Beer, P. D. *Dalton Trans.* **2007**, 1459. (c) Knight, T. E.; Guo, D.; Claude, J. P.; McCusker, J. K. *Inorg. Chem.* **2008**, *47*, 7249. (d) Wong, W. W. H.; Curiel, D.; Cowley, A. R.; Beer, P. D. *Dalton Trans* **2005**, 359. (e) Beer, P. D.; Cheetham, A. G.; Drew, M. G. B.; Fox, O. D.; Hayes, E. J.; Rolls, T. D. *Dalton Trans* **2003**, 603.

(11) (a) Evans, R. C.; Douglas, P.; Winscom, C. J. *Coord. Chem. Rev.* **2006**, *250*, 2093. (b) Balzani, V.; Campagna, S.; Denti, G.; Juris, A.; Serroni, S.; Venturi, M. *Acc. Chem. Res.* **1998**, *31*, 26.

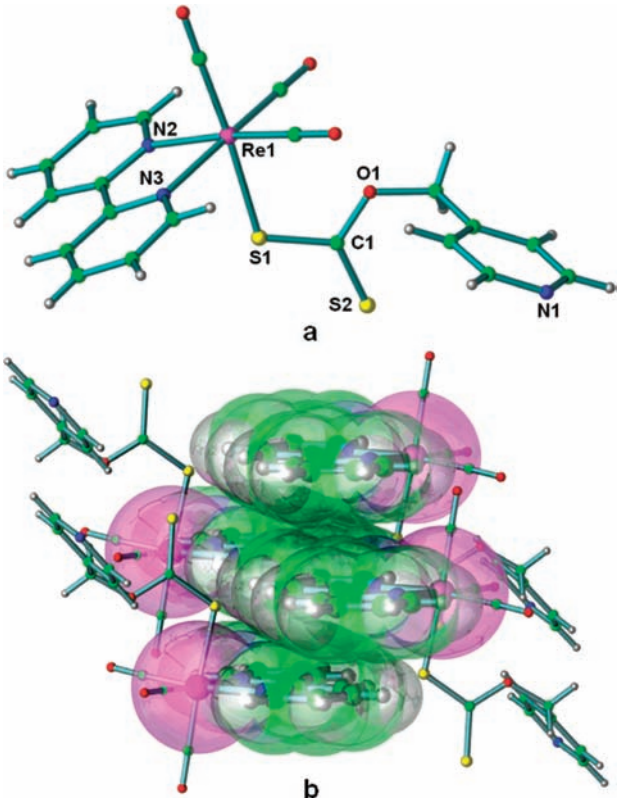

Figure 1. (a) Molecular structure of **1**. Selected bond and angles (Å and deg): Re1−N2 = 2.180(6); Re1−N3 = 2.173(5); Re1−S1 = 2.4905(17); C1−S1 = 1.714(7); C1−S2 = 1.657(7); N2−Re1−N3 = 74.6(2); N2−Re1−S1=83.37(14); N3−Re1−S1=80.84(14). Color code: carbon, green; hydrogen, gray; oxygen, red; nitrogen, blue; rhenium, purple. (b) Space filling representation of the groups involved in the $\pi-\pi$ stacking interactions of **1**.

The crystal packing of **1** is dominated by $\pi-\pi$ stacking interactions of the bipyridine aromatic moieties, as pictured in Figure 1b. One bipyridine ligand overlaps with other symmetry related bipyridine moieties from neighboring molecules, with a perpendicular distance between the rings of 3.48 Å. The rings are parallel positioned (dihedral angle between the rings = 0.0°) and in an offset arrangement, with a slip angle of 29.2°, which is a common orientation of aromatic rings involved in $\pi-\pi$ stacking interactions.[12]

The most important structural characteristic of **1** is the fact that the pyridine end of **L1** is not involved in coordination and is oriented away from the Re(I) center. This feature was designed by us, choosing the Re(I) metallic system with only one vacant coordination site. To test the propensity of **1** to act as a metal-containing ligand in the formation of heterometallic complexes, we selected as a linker between two **L1**-(bipy)$Re(CO)_3$ groups a coordinatively unsaturated Ni(II) dithiophosphonate compound, a species known for its predilection to form adducts with pyridine-based ligands.[13]

Indeed, by mixing dichloromethane solutions of **1** and $[CH_3OCH_2CH_2OP(An)S_2]_2Ni$ ([**Ni**], An = anisole) in a 2:1 ratio, the adduct $[CH_3OCH_2CH_2OP(An)S_2]_2Ni\cdot 2$**L1**(bipy)-$Re(CO)_3$ (**2**) formed in 78% yield. The solution structure of **2** could not be detailed by NMR spectrometry, due to broad peaks, a consequence of the paramagnetic Ni(II) center. However, crystallization of **2** from the same CH_2Cl_2/hexanes system yielded single crystals suitable for X-ray diffraction studies. The compound also crystallizes in the space group $P\bar{1}$, and the asymmetric unit consists of half of a $\{[CH_3OCH_2CH_2OP(An)S_2]_2Ni\}[4\text{-}PyCH_2OCS_2Re(bipy)(CO)_3]_2$ complex (**2**) and one CH_2Cl_2 molecule. The molecular structure of **2** is presented in Figure 2 and consists of a square planar $[CH_3OCH_2CH_2OP(An)S_2]_2Ni$ core, with two $4\text{-}PyCH_2OCS_2Re(bipy)(CO)_3$ molecules axially coordinated to the Ni(II) center through their pyridine groups.

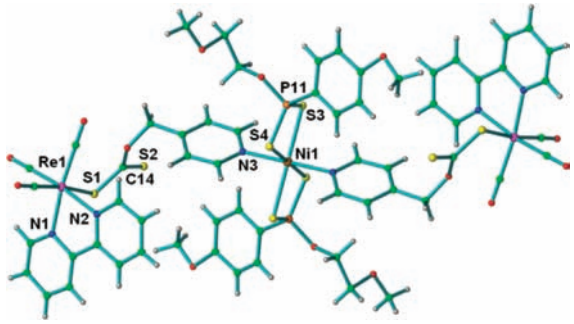

Figure 2. Molecular structure of **2**; selected bond and angles (Å and deg): Re1−N1 = 2.148(7); Re1−N2 = 2.168(8); Re1−S1 = 2.493(2); C14−S1 = 1.713(10); C14−S2 = 1.656(11); Ni1−S3 = 2.503(2); Ni1−S4 = 2.473(3); Ni1−N3 = 2.094(9); P11−S3 = 1.993(4); P11−S4 = 1.995(4); N1−Re1−N2 = 75.3(3); N1−Re1−S1 = 76.7(2); N2−Re1−S1 = 86.0(2); S3−Ni1−S4 = 81.75(9); N3−Ni1−S3 = 89.2(2); N3−Ni1−S4 = 92.7(2). Color code: same as in Figure 1, phosphorus, orange; nickel, brown.

As expected, the coordination of a pyridine group to the Ni(II) center did not influence the structural characteristics of the $-CS_2Re(bipy)(CO)_3$ moiety: the bond lengths and angles for this core in **2** are practically the same as in **1** (see significant data in Figure 2). The NiS_4N_2 core, of D_{2h} local symmetry, exhibits similar coordination patterns as other examples involving 1,1-dithiolate ligands bonded to a Ni(II) center:[13] two PS_2 donor sets are bonded to the Ni(II) center, with Ni−S distances at Ni1−S3 = 2.503(2) Å and Ni1−S4 = 2.473(3) Å, respectively. The P−S distances are practically equal with P11−S3 = 1.993(4) Å and P11−S4 = 1.995(4) Å, respectively. The remaining coordination sites on the Ni(II) center are occupied by two pyridine groups, with equal Ni1−N3 bond lengths of 2.094(9) Å.

The crystal packing of **2** (Figure 3) is governed by a combination of $\pi-\pi$ stacking interactions involving bipyridine and anisole groups: each bipyridine is sandwiched between another bipyridine moiety and an anisole group, both from a neighboring molecule. The rings are parallel positioned and in an offset arrangement, with perpendicular distances between the rings of 3.66 Å (between two bipyridine groups) and 3.41 Å (between a bipyridine and an anisole group). This collection of interactions forms infinite zipper-like chains that propagate along the [101] axis.

The [**Ni**] starting material shows absorption bands at 385, 535, and 695 nm that are attributed to the $^1A_{1\ g}\rightarrow{}^1B_{2g}$, $^1A_g\rightarrow{}^1B_{1g}$, and $^1A_g\rightarrow{}^1B_{1g}$ transitions, respectively (Figure 4 and Table 1).[13c,d] The fourth band around 600 nm ($^1A_g\rightarrow{}^1B_{3g}$) that is also characteristic for square planar Ni(II) complexes is not resolved, being "hidden" by the more intense

(12) Janiak, C. *J. Chem. Soc., Dalton Trans.* **2000**, 3885.
(13) (a) Aragoni, M. C.; Arca, M.; Champness, N. R.; Chernikov, A. V.; Devillanova, F. A.; Isaia, F.; Lippolis, V.; Oxtoby, N. S.; Verani, G.; Vatsadze, S. Z.; Wilson, C. *Eur. J. Inorg. Chem.* **2004**, 2008. (b) Aragoni, M. C.; Arca, M.; Crespo, M.; Devillanova, F. A.; Hursthouse, M. B.; Huth, S. L.; Isaia, F.; Lippolis, V.; Verani, G. *CrystEngComm.* **2007**, *9*, 873. (c) Lebedda, J. D.; Palmer, R. A. *Inorg. Chem.* **1972**, *11*, 484. (d) Gataulina, A. R.; Safin, D. A.; Gimadiev, T. R.; Pinus, M. V. *Trans. Met. Chem.* **2008**, *33*, 921.

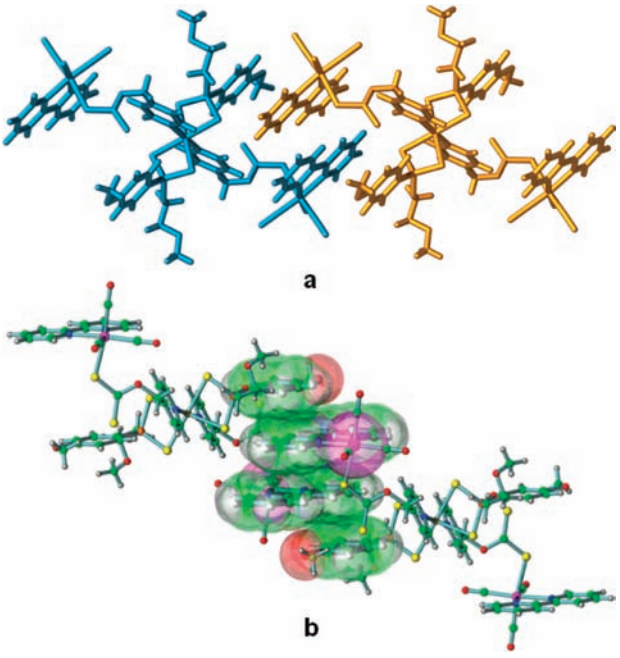

Figure 3. (a) Two interdigitated molecules, generating zipper-like chains. (b) Space filling representation of the groups involved in the $\pi-\pi$ stacking interactions.

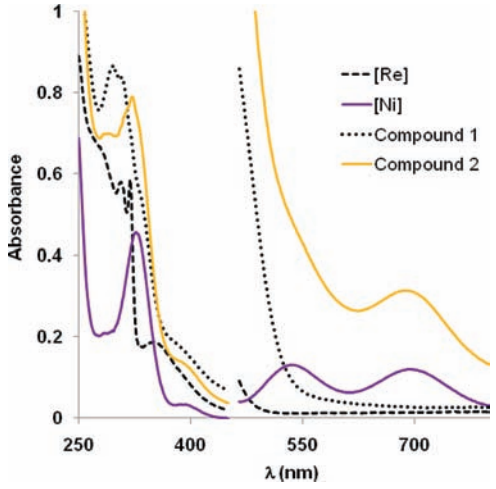

Figure 4. Absorption spectra of **1**, **2**, [**Re**], and [**Ni**] in degassed CH_2Cl_2 at 292 K.

bands at 535 and 695 nm.[13c] The intense high-energy band at 327 nm is assigned to intraligand $\pi\rightarrow\pi^*$ transitions. The electronic absorption spectra of **1** and **2** in degassed CH_2Cl_2 (Figure 4 and Table 1) show absorption bands in the 280−400 nm region. In resemblance to previous spectroscopic studies on similar systems, the low-energy absorption shoulders are attributed to a $d_\pi(Re)\rightarrow\pi^*$(bipy) MLCT transition, while the intense high-energy absorption bands are assigned to intraligand $\pi\rightarrow\pi^*$ transitions.[9,14] A clear difference between **1** and **2** is observed in the visible region; while **1** shows no bands in the 400−800 nm interval, **2** exhibits a band at 690 nm, corresponding to the $^1A_g\rightarrow{}^1B_{1g}$ transition, originating from the Ni(II) chromophore. Excitation of the complexes in

(14) (a) Perkins, T. A.; Humer, W.; Netzel, T. L.; Schanze, K. S. *J. Phys. Chem.* **1990**, *94*, 2229. (b) Lin, R.; Fu, Y.; Brock, C. P.; Guarr, T. F. *Inorg. Chem.* **1992**, *31*, 4346.

Table 1. Absorption and Emission Data for **1**, **2**, [**Re**], and [**Ni**]

	absorption λ_{max}/nm (ε/M^{-1} cm^{-1})	emission λ_{em}/nm	Φ_{em}
1	296 (17 356); 308, sh (16 572); 330, sh (10 295); 374, sh (3334)	544	0.0074
2	287 (56 234); 322 (63 555); 380, sh (10 780); 690 (316)	544	0.0033
[**Re**]	281 (13 278); 305 (11 666); 319 (11 807); 354 (3767)	520	0.0950
[**Ni**]	285 (4189); 327 (9140); 385 (681); 535 (131); 695 (120)		

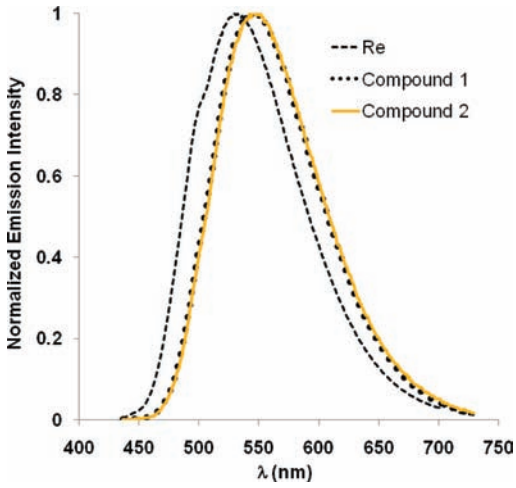

Figure 5. Emission spectra of **1**, **2**, and [**Re**] in degassed CH_2Cl_2 at 292 K.

CH_2Cl_2 solution at $\lambda > 300$ nm resulted in broad emission bands centered at 544 nm, Figure 5. The close resemblance of the emission energies to those reported for related complexes is suggestive of a similar MLCT [$d_\pi(Re)\rightarrow\pi^*$(bipy)] emissive origin.[9,14] The room temperature quantum yields of the xanthate−tricarbonylrhenium complexes **1** and **2** (0.0074 and 0.0033, respectively), while somewhat similar to those of the related rhenium(I) diimine complexes,[9c,15] are much lower than that of the [**Re**] starting material (0.095).

Experimental Section

General Considerations. All operations were carried out under a nitrogen atmosphere using standard Schlenk techniques and a MBraun LabStar drybox. Solvents were dried by conventional methods and distilled under a dry N_2 atmosphere immediately prior to use. Elemental analyses were performed by Robertson Microlit Laboratories. NMR spectra were recorded by using a 400 MHz Bruker Avance FT-NMR Spectrometer. UV−vis and fluorescence spectra were recorded on a Shimadzu UV-3100 Spectrophotometer and on an Aminco-Bowman Luminescence Spectrometer, respectively. Luminescence quantum yield was measured by the optically dilute method,[16a] using a degassed solution of $[Ru(bipy)_3]_2^+$ in dichloromethane (Φ_{em} = 0.029) as a reference.[16b] All reagents are commercially available (Sigma-Aldrich or Pressure Chemical Co.) and were used without further purification. $CH_3OCH_2CH_2OP(An)S_2NH_4$ (An = anisole) was prepared using the classic synthetic procedure for

(15) (a) Sun, S.-S.; Lees, A. J. *Organometallics* **2002**, *21*, 39. (b) Xue, W.-M.; Goswami, N.; Eichhorn, D. M.; Orizondo, P. L.; Rillema, D. P. *Inorg. Chem.* **2000**, *39*, 4460. (c) Yam, V. W.-W.; Lau, V. C.-Y.; Cheung, K.-K. *Organometallics* **1996**, *14*, 2749.

(16) (a) Demas, J. N.; Crosby, G. A. *J. Phys. Chem.* **1971**, *75*, 991. (b) Caspar, J. V.; Meyer, T. J. *J. Am. Chem. Soc.* **1983**, *105*, 5583.

this type of compound: a mixture of 2-methoxyethanol and 2,4-bis(4-methoxyphenyl)-1,3-dithia-2,4-diphosphetane-2,4-disulfide (Lawesson's Reagent) in a 2 to 1 ratio was refluxed in benzene for 1 h. Passing a stream of dry, gaseous ammonia through the clear solution produced in practically quantitative yield the ammonium dithiophosphonate salt $CH_3OCH_2CH_2OP(An)S_2NH_4$ as a white, voluminous precipitate which was filtered, washed with benzene and ether, and air-dried.

4-PyCH$_2$OCS$_2$Na (L1). 4-Pyridylcarbinol (1.09 g, 10 mmol) was dissolved in dry THF (50 mL) and added dropwise to a suspension of NaH (0.24 g, 10 mmol) in dry THF (100 mL) under an inert atmosphere at −20 °C in a salt-ice bath. The mixture was stirred for 20 min; then, excess carbon disulfide (1.0 mL, 1.6 excess) was added dropwise, and the resulting mixture was stirred for 1 h while allowed to return to room temperature. The yellow solution was filtered to remove any solid impurities, and then the THF was removed under reduced pressure. The resulting yellow powder was dried under a vacuum; the solid (1.93 g, yield 93.1%) was identified as 4-PyCH$_2$OCS$_2$Na (**L1**). ^{1}H NMR (acetone-d$_6$): δ: 8.50 (d, J = 13.8 Hz, 2H, *Py*), 7.37 (d, J = 13.8 Hz, 2H, *Py*), 5.59 (s, 2H, Py-CH_2); MS (ESI$^-$) m/z for $C_7H_6NOS_2^-$ [M$^-$]: 184. Anal. Calcd for $C_7H_6NNaOS_2$: C = 40.57, H = 2.92, N = 6.76. Found: C = 40.81, H = 3.25, N = 6.91.

[Re(bipy)(CO)$_3$(NCCH$_3$)](O$_3$SCF$_3$) ([Re]). Following published synthetic procedures,[17] the [**Re**] starting material was prepared as a yellow poweder in 78% overall yield. ^{1}H NMR (acetone-d$_6$): δ 9.23 (d, J = 5.4 Hz, 2H, *bipy*), 8.87 (d, J = 8.4 Hz, 2H, *bipy*), 8.50 (t, J = 7.9 Hz, 2H, *bipy*), 7.95 (m, 2H, *bipy*). UV−vis absorption spectrum, λ_{max}/nm (ε/M^{-1} cm^{-1}): 281 (13 278); 305 (11 666); 319 (11 807); 354 (3767).

4-PyCH$_2$OCS$_2$Re(bipy)(CO)$_3$ (1). [Re(bipy)(CO)$_3$(NCCH$_3$)](O$_3$SCF$_3$) (0.103 g, 16.7 mmol) was dissolved in acetone (25 mL) and added to a solution of **L1** (0.035 g, 16.8 mmol) in acetone (50 mL) and stirred at room temperature for two days. The acetone was removed under reduced pressure, and the resulting orange solid was redissolved in CH_2Cl_2. The insoluble NaOTf and unreacted **L1** were removed by filtration; removal of CH_2Cl_2 under reduced pressure yielded compound **1** (0.083 g, yield 82.1%) as an orange powder. ^{1}H NMR (acetone-d$_6$): δ 9.11 (d, J = 5.4 Hz, 2H, *bipy*), 8.74 (d, J = 8.6 Hz, 2H, *bipy*), 8.54 (d, J = 6.3 Hz, 2H, *py*), 8.34 (t, J = 8.6 Hz, 2H, *bipy*), 7.74 (m, 2H, *bipy*), 7.28 (d, J = 6.3, 2H, *py*), 5.61 (s, 2H, Py-CH_2). MS (ESI$^+$) m/z for $C_{20}H_{15}N_3O_4ReS_2^+$ [M + H]$^+$: 612. Anal. Calcd. for $C_{20}H_{14}N_3O_4ReS_2$: C = 39.34, H = 2.31, N = 6.88. Found: C = 38.98, H = 2.25, N = 6.78. UV−vis absorption spectrum, λ_{max}/nm (ε/M^{-1} cm^{-1}): 296 (17 356); 308, sh (16 572); 330, sh (10 295); 374, sh (3334).

[CH$_3$OCH$_2$CH$_2$OP(An)S$_2$]$_2$Ni ([Ni]). A 250 mL flask was charged with a stirring bar and an aqueous solution of $NiCl_2\cdot 6H_2O$ (1.188 g, 5 mmol in 75 mL water). To this solution was added an aqueous solution of $CH_3OCH_2CH_2OP(An)S_2NH_4$ (2.954 g, 10 mmol in 75 mL water). Upon stirring overnight, a purple precipitate formed which was filtered off, washed with 100 mL of water, and dried in open air, yielding 2.62 g (85.4%) of the desired compound. Anal. Calcd for $C_{20}H_{28}NiO_6P_2S_4$: C = 39.17, H = 4.60. Found: C = 39.44, H = 4.21. UV−vis absorption spectrum, λ_{max}/nm (ε/M^{-1} cm^{-1}): 285 (4189); 327 (9140); 385 (681); 535 (131); 695 (120).

{[CH$_3$OCH$_2$CH$_2$OP(An)S$_2$]$_2$Ni}[4-PyCH$_2$OCS$_2$Re(bipy)(CO)$_3$]$_2$ (2). A 100 mL flask was charged with a stirring bar, [CH$_3$OCH$_2$CH$_2$OP(An)S$_2$]$_2$Ni (0.040 g, 0,065 mmol), and 4-PyCH$_2$OCS$_2$Re(bipy)(CO)$_3$ (0.080 g, 0.13 mmol). The addition of 50 mL of dichloromethane produced a clear dark yellow solution that turned orange over a period of 4 days of stirring. Removal of the solvent yielded compound **2** (0.094 g, yield 78.3%) as an orange powder. ^{1}H NMR (acetone-d$_6$), all broad: δ 8.47, 8.21, 7.96, 7.34, 6.99, 6.89, 4.81. MS (ESI$^+$) m/z for $C_{60}H_{57}N_6NiO_{14}P_2Re_2S_8^+$, [M + H]$^+$: 1834. Anal. Calcd for $C_{60}H_{56}N_6NiO_{14}P_2Re_2S_8$: C = 39.28, H = 3.08, N = 4.58. Found: C = 39.75, H = 3.45, N = 4.62. UV−vis absoption spectrum, λ_{max}/nm (ε/M^{-1} cm^{-1}): 287 (56 234); 322 (63 555); 380, sh (10 780); 690 (316).

Table 2. Crystal Data and Structure Refinement for **1** and **2**

	1·1/2 CH_2Cl_2	**2**· CH_2Cl_2
empirical formula	$C_{20.50}H_{15}ClN_3O_4ReS_2$	$C_{61.80}H_{43.60}Cl_{3.60}N_6NiO_{14}P_2Re_2S_8$
FW, g mol^{-1}	653.13	1971.63
cryst syst	triclinic	triclinic
space group	$P\bar{1}$	$P\bar{1}$
T (K)	150(2)	100(2)
a (Å)	6.4657(5)	8.6958(2)
b (Å)	13.0464(11)	13.2303(3)
c (Å)	14.5100(12)	16.6336(3)
α (deg)	112.213(2)	90.417(2)
β (deg)	99.322(2)	98.010(2)
γ (deg)	90.503(2)	98.877(2)
V (Å^3)	1114.89(16)	1871.48(7)
Z	2	1
R_1; $I > 2\sigma(I)$	0.0370	0.0596
wR_2; $I > 2\sigma(I)$	0.0825	0.1548

Crystal Structure Determinations. Single crystals of **1** were obtained by layering with hexanes a dichloromethane solution of **1**. X-ray intensity data from a yellow needle crystal were measured at 150(2) K on a Bruker SMART APEX diffractometer (Mo Kα radiation, λ = 0.71073 Å).[18] Raw area detector data frame integration was performed with SAINT+.[18] Final unit cell parameters were determined by least-squares refinement of 3414 reflections from the data set. The data were corrected for absorption effects with SADABS.[18] Direct methods structure solution, difference Fourier calculations, and full-matrix least-squares refinement against F^2 were performed with SHELXTL.[19] The compound crystallizes in the space group $P\bar{1}$ of the triclinic system. The asymmetric unit consists of one 4-PyCH$_2$OCS$_2$Re(bipy)(CO)$_3$ complex and half of a CH_2Cl_2 molecule which is disordered about an inversion center. Atom Cl1 of the CH_2Cl_2 molecule is located on the inversion center. Cl2 and C21 atom site occupancies initially refined to near 0.5 and were subsequently fixed at that value for the final cycles. C−Cl distances were restrained to be approximately equal. All non-hydrogen atoms were refined with anisotropic displacement parameters. Hydrogen atoms were placed in geometrically idealized positions and included as riding atoms. The largest residual difference map extrema are located < 1 Å from Re1.

Single crystals of **2** were obtained by layering with hexanes a dichloromethane solution of **2**. X-ray intensity data from a clear intense yellow prism were measured at 100(2) K on a Bruker SMART APEXII diffractometer (Cu Kα radiation, λ = 1.54184 Å).[20] Raw area detector data frame integration was performed with Saint+.[20] Final unit cell parameters were determined by least-squares refinement of 21 760 reflections from the data set. The data were corrected for absorption effects with SADABS.[20] Direct methods structure solution, difference Fourier calculations, and full-matrix least-squares refinement against F^2 were performed with Shelxl.[21] The compound crystallizes in space group $P\bar{1}$ of the triclinic system. The asymmetric unit consists of one-half of a {[CH$_3$OCH$_2$CH$_2$OP(An)S$_2$]$_2$Ni}[4-PyCH$_2$OCS$_2$Re(bipy)(CO)$_3$]$_2$ complex, with the nickel(II)

(17) Fredericks, S. M.; Luong, J. C.; Wrighton, M. S. *J. Am. Chem. Soc.* **1979**, *101*, 7415.

(18) *SMART*, version 5.630; *SAINT+*, version 6.45; *SADABS*, version 2.10; Bruker Analytical X-ray Systems, Inc.: Madison, WI, 2003.

(19) Sheldrick, G. M. *SHELXTL*, version 6.14; Bruker Analytical X-ray Systems, Inc.: Madison, WI, 2000.

(20) *APEX2*, version 2009.3−0; *Saint+*, version V7.56A; *SADABS*, version 2008/1; Bruker Analytical X-ray Systems, Inc.: Madison, WI, 2008.

(21) Sheldrick, G. M. *Acta Crystallogr.* **2008**, *A64*, 112–122.

Table 3. Selected Bond Lengths (Å) and Angles (deg) for **1** and **2**

1·1/2 CH_2Cl_2		**2**· CH_2Cl_2	
Re(1)−C(19)	1.905(8)	Re1−C11	1.917(9)
Re(1)−C(20)	1.920(8)	Re1−C12	1.913(11)
Re(1)−C(18)	1.925(8)	Re1−C13	1.953(11)
Re(1)−N(3)	2.173(5)	Re1−N1	2.148(7)
Re(1)−N(2)	2.180(6)	Re1−N2	2.168(8)
Re(1)−S(1)	2.4905(17)	Re1−S1	2.493(2)
S(1)−C(1)	1.714(7)	S1−C14	1.713(10)
S(2)−C(1)	1.657(7)	S2−C14	1.656(11)
C(1)−O(1)	1.348(8)	O4−C14	1.346(12)
C(2)−O(1)	1.435(8)	O4−C15	1.446(12)
		Ni1−S3	2.503(2)
		Ni1−S4	2.473(3)
		Ni1−N3	2.094(9)
		S3−P11	1.993(4)
		S4−P11	1.995(4)
C(19)−Re(1)−C(20)	89.0(3)	C11−Re1−C12	89.5(4)
C(19)−Re(1)−C(18)	88.4(3)	C12−Re1−C13	88.9(5)
C(20)−Re(1)−C(18)	89.9(3)	C11−Re1−C13	89.2(4)
N(3)−Re(1)−N(2)	74.6(2)	N1−Re1−N2	75.3(3)
C(19)−Re(1)−N(3)	99.4(2)	N1−Re1−C11	96.1(3)
C(20)−Re(1)−N(3)	169.8(2)	N1−Re1−C13	172.7(4)
C(18)−Re(1)−N(3)	96.1(2)	N1−Re1−C12	96.1(4)
C(19)−Re(1)−N(2)	173.7(2)	N2 −Re1-C12	171.1(4)
C(20)−Re(1)−N(2)	96.8(2)	N2−Re1−C13	99.5(4)
C(18)−Re(1)−N(2)	94.0(3)	N2−Re1−C11	93.4(3)
N(3)−Re(1)−S(1)	80.84(14)	S1−Re1−N1	76.7(2)
N(2)−Re(1)−S(1)	83.37(14)	S1−Re1−N2	86.0(2)
		S3−Ni1−S4	81.75(9)
		S3−Ni1−N3	89.2(2)
		S4−Ni1−N3	92.7(2)
		Ni1−S3−P11	83.93(12)
		Ni1−S4−P11	84.69(12)
		S3−P11−S4	109.48(16)

center positioned upon an inversion center. The pendant $CH_3OCH_2CH_2O$ group is disordered over two sites (75:25). A solvent molecule of CH_2Cl_2 was located in a difference density map and refined to a site occupancy of 90%. Bond distances C30−Cl1/C30−Cl2, C28−07/C28−O7a, and C29−O7/C29a−O7a were restrained to be approximately equal. All non-hydrogen atoms were refined with anisotropic displacement parameters with the exception of O5, O7, O7a, C29, C29a, and C31 atoms refined with an isotropic model. Hydrogen atoms were placed in geometrically idealized positions and included as riding atoms. The largest residual difference map extrema are located <1 Å from Re1.

Details about crystal data collection and refinement parameters for **1** and **2** are collected in Table 2, while selected bond distances and angles are given in Table 3.

Conclusions

In conclusion, we described here a simple, high-yield stepwise approach toward heterometallic complexes, based on a pyridine functionalized xanthate ligand. This strategy, built on applying the HSAB principles to the O-alkyldithiocarbonate donor system, is easily transferable to other 1,1-dithiolate systems and can be used in combination with a large variety of luminescent metallic systems. We are currently expanding this study using also the dithiophosphonate donor set and investigating the insertion of two different luminescent metallic centers within the same molecule, results that will be presented in a forthcoming paper.

Acknowledgment. This work is dedicated to Professor Ionel Haiduc on the occasion of his 73rd birthday. The authors thank Eastern Illinois University for a CFR seed grant. The Bruker APEX II CCD Single Crystal Diffractometer at Eastern Illinois University was purchased using funds provided by the NSF through Grant CHE-0722547.

Supporting Information Available: UV−vis spectra of all compounds and X-ray crystallographic data of complexes **1** and **2** in CIF format. This material is available free of charge via the Internet at http://pubs.acs.org.